Articles

Structural Influence of Cation Binding to Recombinant Human Brain S100b: Evidence for Calcium-Induced Exposure of a Hydrophobic Surface†

Steven P. Smith, Kathryn R. Barber, Stanley D. Dunn, and Gary S. Shaw*

Department of Biochemistry and McLaughlin Macromolecular Structure Facility, The University of Western Ontario, London, Ontario, Canada, N6A 5C1

Received November 10, 1995; Revised Manuscript Received May 1, 1996⊗

ABSTRACT: The dimeric calcium-binding protein S100b is proposed to undergo a calcium-induced structural change allowing it to interact, via a hydrophobic surface, with other proteins. Previously it has been suggested that calcium binding to S100b leads to the exposure of at least one phenylalanine residue (Mani et al., 1982, 1983). This effect appears to be "reversed" at higher ionic strength, leading to a possible reburying of phenylalanine residues (Mani et al., 1982, 1983). To study these effects, we monitored calcium binding to recombinant human S100b by NMR spectroscopy under different salt (KCl) conditions. ^{15}N-Labeled glycine residues in S100b showed calcium-induced chemical shift changes similar to those reported for the related monomeric protein calbindin D_{9k}, suggesting similar conformational changes are occurring in the calcium-binding loops of these two proteins. Calcium binding to S100b also resulted in a shifting and broadening of several ^{1}H resonances from the Ca-S100b form only including those from the side chains of residues F14, F70, and F73 but not those of residue Y17. This broadening was enhanced with increased ionic strength (KCl). However, small additions (<15% v/v) of the hydrophobic solvent trifluoroethanol relieved this phenomenon, leading to narrower line widths. These observations are consistent with the calcium-induced exposure of at least one of these hydrophobic residues, resulting in self-association of the S100b dimer. Trifluoroethanol serves to dissociate these complexes back to the dimeric calcium species. We propose that this cluster of hydrophobic residues which include F14, F73, and F88 may be important for interactions with a target protein.

Calcium-binding proteins are involved in many biochemical processes including vision, muscle contraction, neurotransmitter release, enzyme regulation and cellular calcium buffering. One major family of calcium-binding proteins which span many of these functions are the EF-hand proteins. For example, proteins such as troponin-C and calmodulin bind calcium and modulate muscle contraction and enzymatic activity, respectively, while others like parvalbumin and calbindin D_{9k} are thought to buffer intracellular calcium concentration. These two broad functional categories of EF-hand proteins have also been described on a structural level from a wealth of three-dimensional studies of apo- and calcium-bound troponin-C (Gagne et al., 1994; 1995; Herzberg & James, 1988; Satyshur et al., 1988, 1994), calbindin D_{9k} (Akke et al., 1992; Kordel et al., 1993; Skelton et al., 1995; Szebenyi & Moffat, 1986), and calmodulin (Babu et al., 1988; Finn et al., 1995; Kuboniwa et al., 1995; Zhang et al., 1995a). It has been observed that calcium-modulating proteins such as troponin-C and calmodulin undergo a significant conformational change upon calcium binding in order to interact with target proteins and modulate their biological effects (Gagne et al., 1995; Zhang et al., 1995a). On the other hand, calcium-buffering proteins, such as calbindin D_{9k} and parvalbumin, exhibit only small changes in tertiary structure in response to calcium binding (Skelton et al., 1994; Williams et al., 1986).

One group of EF-hand calcium-binding proteins where little tertiary structural information is available are the S100 proteins. This family of proteins comprises about 15 members including S100a and S100b, calcyclin, p11, calbindin D_{9k}, and the calgranulins (Hilt & Kligman, 1991). Some initial insight into the three-dimensional structures of these proteins has recently been provided from the low-resolution structure of apo-calcyclin which may serve as a template for all S100 proteins (Potts et al., 1995). The proteins are acidic dimers, ranging in size from 20 to 24 kDa, and are generally expressed in a cell-specific manner (Hilt & Kligman, 1991). One exception is the 75-amino acid protein calbindin D_{9k}, which has a shorter C-terminal sequence and exists as a monomer in solution. S100b is one of the best characterized of the S100 proteins and is composed of two 91-residue β subunits, each containing two calcium-binding sites (Isobe & Okuyama, 1981). The C-terminal sequence of S100b contains a canonical 12-residue EF-hand calcium-binding loop (residues 61−72) comprised largely of acidic residues. However, the N-terminal calcium-binding loop (residues 18−31) is mostly

† This research was supported by a grant from the Medical Research Council of Canada (G.S.S.) and a graduate studentship from the Alzheimer Society of London (S.P.S). Funding for the NMR spectrometer in the McLaughlin Macromolecular Structure Facility was made possible through grants from the Medical Research Council of Canada and the Academic Development Fund of The University of Western Ontario and generous gifts from the R. Samuel McLaughlin Foundation and London Life Insurance Co. of Canada.

* Author to whom correspondence should be addressed.

⊗ Abstract published in *Advance ACS Abstracts,* June 15, 1996.

S0006-2960(95)02698-5 CCC: $12.00

basic in nature and contains 14 residues (Hilt & Kligman, 1991). In S100 proteins, the C-terminus of the protein is the most variable in sequence and has been suggested to be important in the function of these proteins. While this specific biological function has not been confirmed for S100b, intracellular roles have been proposed. *In vitro* studies have indicated that S100b acts to inhibit the calcium-dependent phosphorylation of several neurospecific proteins including tau, MARCKS,[1] and GAP43 (Baudier et al., 1987; Lin et al., 1994; Sheu et al., 1995). S100b has also been shown to control the assembly or association of larger protein complexes (p53, microtubules, and GFAP) (Baudier et al., 1992; Bianchi et al., 1993; Donato, 1988). Recently, it has been shown using a bacteriophage random peptide library that S100b binds to a protein resembling the actin capping protein, CapZ, in a calcium-dependent manner (Ivanenkov et al., 1995). These observations are consistent with S100b acting as a modulating protein which undergoes a calcium-dependent conformational change in order to interact specifically with these other proteins.

At physiological pH, the S100b dimer binds two calcium ions ($K_d \approx 7-50$ μM) (Baudier et al., 1986b; Mani et al., 1983). Circular dichroism studies have shown that apo-S100b is mostly α-helical (55%) but surprisingly undergoes a 10−15% decrease in θ_{222} upon calcium binding (Mani et al., 1983), suggesting an apparent loss in α-helical structure. Fluorescence and absorption difference studies have indicated that calcium binding to S100b allows Y17 in the N-terminal region of the protein to move to a more nonpolar environment while at least one of the seven phenylalanine residues (per monomer) becomes exposed to solvent (Mani et al., 1982, 1983). Further, calcium binding to S100b leads to the exposure of two sulfhydryls per dimer, an increase in TNS fluorescence, and modulation of binding to phenyl-Sepharose (Baudier & Gerard, 1983; Baudier et al., 1984, 1985). These results are all consistent with the calcium-induced exposure of a hydrophobic surface in S100b, similar to that observed for troponin-C and calmodulin (Gagne et al., 1995; Zhang et al., 1995a), which may be important for interaction with proteins such as MARCKS, tau, and GFAP.

While calcium binding studies point toward a calcium-induced structural change in S100b, there is no clear evidence of where this change occurs, nor of its magnitude. In addition, S100b exhibits an unusual behavior toward monovalent ions, and calcium binding to S100b is significantly antagonized by increased potassium concentrations such that at physiological KCl concentrations (120 mM) the calcium affinity of S100b is greatly reduced ($K_d \approx 1$ mM) (Baudier & Gerard, 1983; Mani et al., 1982). ^{43}Ca NMR experiments have shown that this antagonistic effect is not due to competitive binding of potassium and calcium ions (Ogoma et al., 1992). Other spectroscopic studies show that potassium ions modify the environment of at least one phenylalanine residue and increase the ellipticity at 222 nm of the calcium-bound form of S100b (Mani et al., 1982). This antagonistic influence of potassium ions on calcium binding to S100b has raised some doubts as to the role of S100b as a calcium-modulating protein although the details of the structural effects of potassium ions on S100b have not been investigated. In this work, we describe the overexpression and purification of recombinant human S100b and use high-resolution NMR spectroscopy to identify the effect of potassium on S100b in the absence and presence of calcium. Our results suggest that increased ionic strength results in self-association of Ca-S100b, a result of the exposure of some hydrophobic residues including F14 and F73.

MATERIALS AND METHODS

Rat S100b cDNA was graciously supplied by R. Dunn at Montreal General Hospital Research Institute. Two plasmids, pHSB67-1 and pHSB67-2, containing the upstream and downstream segments of the full-length human S100b cDNA were generously donated by R. Kuwano at Niigata University, Japan. $^{15}NH_4Cl$, [^{15}N]glycine, imidazole-d_4, and deuterium oxide were obtained from Isotec Inc. (Miamisburg, OH). Puratronic grade calcium chloride (99.9975%) was obtained from Aesar/Johnson Matthey (Brampton, Ontario, Canada). The auxotrophic bacterial strain DL39 GlyA λDE3 (LeMaster & Richards, 1988) used for specific amino acid labeling was kindly supplied by L. McIntosh at the University of British Columbia. All other chemicals used were of the highest purity commercially available.

Plasmid Construction. The cloning plasmid pHN2 (Patel & Dunn, 1995) contains a *tac* promoter upstream of the multiple cloning site, the *unc* terminator inserted into the *Hind*III site at the downstream end of the multiple cloning site, and the lacI^q gene carried elsewhere on the plasmid. pHN2 was partially digested with *Hind*III, ends were filled, and the plasmid was religated. One of the resultant plasmids, termed pSD80, had only the *Hind*III site downstream from the unc terminator removed while the *Hind*III site upstream from the unc terminator remained intact. Recombinant DNA procedures were carried out by standard methods (Sambrook et al., 1989).

Using the upstream primer CGCGGAATTCTGGAGGATTTTAAAATGTCTGAGCTTGAGAAGGCCATGGTTGCCC and PCR, a 37-bp segment containing an *Eco*RI site, a Shine−Delgarno sequence, and nucleotides encoding the first five amino acids of rat S100b protein was added to the 5′ end of the rat S100b cDNA. A 12-bp segment containing a stop codon and a *Pst*I site was also added to the 3′ end of the rat S100b cDNA. This 299-bp *Eco*RI−*Pst*I-digested rat S100b cDNA fragment was inserted into the *Eco*RI and *Pst*I sites of the cloning region of pSD80, resulting in the formation of pSS1.

A 110-bp fragment of pHSB67-1 corresponding to the 5′ portion of the human S100b cDNA was purified after the plasmid had been digested with *Sac*I and *Eco*RI. pHSB67-2 was cut with *Eco*RI and *Hind*III, resulting in a 179-bp fragment containing the 3′ portion of the human S100b cDNA. These two fragments were inserted into pSS1, which had been cut with *Sac*I and *Hind*III, via a three-component ligation to produce pSS2. The plasmid was maintained and expressed in *Escherichia coli* strain N99.

Expression and Purification of Human S100b. E. coli N99/pSS2 was grown in 1 L of LB media supplemented with

[1] Abbreviations: PCR, polymerase chain reaction; IPTG, isopropyl β-D-thiogalactopyranoside; EDTA, ethylenediaminetetraacetic acid, disodium salt; DTT, DL-dithiothreitol; ICP, inductive coupled plasma spectroscopy; HSQC, heteronuclear single quantum correlation; DSS, 3-(trimethylsilyl)-1-propanesulfonic acid; NMR, nuclear magnetic resonance; SDS, sodium dodecyl sulfonate; TFE, trifluoroethanol; TNS, 6-(*p*-toluidino)naphthalene-2-sulfonic acid; MARCKS, myristoylated alanine-rich C kinase substrate; GFAP, glial fibrillary acidic protein; apo-S100b, calcium-free S100b; Ca-S100b, calcium-bound S100b; HyTEMPO, 4-hydroxy-2,2,6,6-tetramethylpiperidinyl-1-oxy.

40 mg/L carbenicillin in a 2.8 L Fernbach flask at 37 °C with vigorous shaking. When A_{600} reached 0.7, 1 mM IPTG was added, and growth was continued for 3−4 h. The cells were harvested by centrifugation, washed once with 50 mM Tris-HCl, pH 8.0, 5 mM $MgCl_2$, and stored frozen at −80 °C. All fractionation steps were performed at 4 °C. Cells were resuspended in a volume of 50 mM Tris-HCl, pH 8.0, 5 mM $MgCl_2$ equal to 10 times their packed weight, and then disrupted by one passage through the French pressure cell at 20 000 psi. Cell debris was removed by centrifugation for 15 min at 10 000 rpm in a Beckman JA-20 rotor. The supernatant solution was centrifuged for 2 h at 38 000 rpm in a Beckman Ti-50 rotor. The supernatant solution was collected, and ammonium sulfate was added, with stirring, to bring it to 90% of saturation. After the supernatant was collected, the pH was adjusted to 4 by the addition of 10% (v/v) orthophosphoric acid and stirred at 4 °C for an additional 30 min. The precipitate was collected by centrifugation at 10 000 rpm for 15 min, redissolved in 25 mM Tris-HCl, pH 8.0, 1 mM EDTA, and 1 mM DTT, and dialyzed overnight against the same buffer.

The dialyzed sample was applied to a MonoQ anion exchange column (Pharmacia) attached to a Waters 625 LC HPLC unit. The column was equilibrated in 100% (v/v) buffer A (25 mM Tris-HCl, pH 8.0, 1 mM EDTA, and 1 mM DTT), and elution was monitored at 270 nm with a flow rate of 1 mL/min. The following linear gradient program was used: 0 min, buffer A = 100%; 30 min, buffer A = 0%, buffer B = 100% (25 mM Tris-HCl, pH 8.0, 1 mM EDTA, 1 mM DTT, and 1 M NaCl). S100b eluted at 0.43 M NaCl and appeared as a single band on SDS−polyacrylamide gel electrophoresis. The purity of the protein was confirmed by electrospray mass spectrometry analysis.

^{15}N Labeling of Human S100b. Uniformly ^{15}N-labeled human S100b was obtained by growing *E. coli* N99/pSS2 in M9 minimal media (Sambrook et al., 1989) using $^{15}NH_4Cl$ (0.75 g/L) as the sole nitrogen source. Bacteria were grown at 37 °C with vigorous shaking. At $A_{600} = 0.17$, IPTG was added to 1 mM. Incubation at 37 °C with aeration and vigorous shaking was continued for 14 h, at which time the cells were harvested. Selective ^{15}N-labeling of human S100b was achieved by growing *E. coli* DL39 GlyA λDE3/pSS2 on M9 minimal media supplemented with ^{15}N-labeled glycine (400 mg/L) and a mixture of 18 unlabeled amino acids lacking serine (Muchmore et al., 1989). 1 mM IPTG was added at an $A_{600} = 0.5$, and growth was continued at 37 °C with aeration and vigorous shaking for an additional 5−6 h. A concentration of 40 mg/L of carbenicillin was used for both labeling procedures. The purification of the uniformly labeled and selectively labeled human S100b followed the same protocol as described above for unlabeled human S100b. Preparation of the apo form of the protein entailed dialysis against 50 mM KCl, pH 8.0, 3 mM EDTA followed by extensive dialysis against 50 mM KCl, pH 8.0, to remove the EDTA. After final dialysis against 3 mM KCl, pH 8.0, the protein was freeze-dried.

Sample Preparations for NMR Studies. NMR samples containing apo-S100b were adjusted to pH 7.0−7.1 by the addition of 10% (v/v) DCl or 10% (w/v) KOD. Protein concentrations were determined in triplicate by amino acid analysis by comparing alanine and leucine peak areas to those of a standard 6.25 nmol sample. A 5.15 nmol norleucine internal standard was added to both the standard and protein samples. A calcium stock solution (500.5 mM) was prepared in D_2O, and its calcium content was determined in triplicate by ICP analysis. Dilute calcium solutions (50 and 125 mM) were prepared from this stock solution in D_2O, and additions (1−5 μL) were made directly to the NMR tube using a calibrated 10 μL Hamilton syringe. All NMR samples contained a 5-fold molar excess of DTT-d_{10} versus protein (except HyTEMPO experiments). Appropriate amounts of TFE-d_3 were added to the samples which would give rise to a TFE concentration of 10% (v/v).

Lyophilized human apo-S100b was dissolved in 500 μL of a buffer containing 30 mM imidazole-d_4 in D_2O (99.996%) for one-dimensional ^1H NMR KCl and TFE titration studies both in the presence and in the absence of calcium. For the ^1H and $^1H-^{15}N$ HSQC calcium titration experiments, lyophilized [^{15}N]glycine labeled human S100b was dissolved in 500 μL of buffer containing 20 mM imidazole-d_4 in 90% H_2O and 10% D_2O. Uniformly ^{15}N-labeled human S100b protein used in $^1H-^{15}N$ HSQC experiments was dissolved in 500 μL of 90% H_2O and 10% D_2O. For experiments utilizing HyTEMPO, 1−2 μL additions of the spin-label in a 20 mM imidazole-d_4 solution were made directly to the NMR sample (Petros et al., 1990; Esposito et al., 1992).

NMR Spectroscopy. All the NMR spectra were acquired on a Varian Unity 500 spectrometer equipped with a pulsed field gradient (PFG) triple-resonance probe at 35 °C. ^1H NMR experiments monitoring the concentration effects of KCl and TFE on apo- and calcium-bound S100b used the following acquisition parameters: spectral width = 5999.7 Hz, 90° pulse width = 11.5 μs, acquisition time = 2.0 s. Suppression of the H_2O (or HDO) resonance was accomplished with use of a 2.0 s. presaturation pulse. All spectra were referenced to the trimethylsilyl resonance of DSS at 0.0 ppm.

$^1H-^{15}N$ HSQC spectra of the uniformly ^{15}N-labeled and [^{15}N]glycine-labeled human S100b samples were collected using the sensitivity enhanced method (Kay et al., 1992). The number of complex data points, acquisition times, and carrier frequencies were, respectively: 1024, 64 ms, 4.73 ppm (^1H); 128, 21.3 ms, 120.00 ppm (^{15}N).

RESULTS

Protein Expression and Purification. Ligation products were sequenced to identify which resultant plasmids contained the full-length human S100b cDNA in the proper orientation. Expression of recombinant human S100b protein in cells containing the plasmid pSS2 was induced via the addition of IPTG, as described under Materials and Methods. Purification of human S100b was a simplified version of a previous method (VanEldik et al., 1988). The purification procedure was monitored by SDS−PAGE (Figure 1). Solubilized cell extract contained an intense band which migrated similarly to bovine brain S100b (Figure 1, lane 7). After 90% ammonium sulfate saturation, the protein was isoelectric-precipitated at pH 4. Resolubilization of the pellet at pH 8 showed that the protein appeared as a single band (Figure 1, lane 5). Subsequent anion exchange chromatography was used to further purify recombinant human S100b to homogeneity (Figure 1, lane 6). This species was verified to be human S100b by electrospray mass spectrometry which showed the protein was a 50:50 mixture of species either bearing (monomer MW_{obs} 10 739.0, MW_{calc} 10 739.7) or

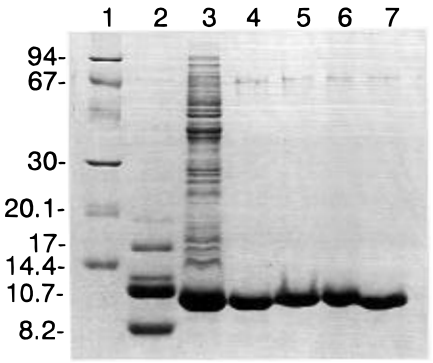

FIGURE 1: Purification of recombinant human S100b monitored by 20% SDS−PAGE. Lane 1, low molecular weight protein standard; lane 2, CNBr-digested sperm whale myoglobin standard; lane 3, cell lysate (37 °C, 9 h); lane 4, 90% ammonium sulfate supernatant; lane 5, redissolved pH 4 pellet; lane 6, anion exchange HPLC fraction; lane 7, bovine S100b. Approximate molecular weights derived from the molecular weight standards (lanes 1 and 2) are shown to the left of the figure.

lacking (monomer MW_{obs} 10 713.0, MW_{calc} 10 712.7) the *N*-formyl group on the N-terminal methionine residue.

Calcium-Induced Conformational Changes in S100b. The conformational response of recombinant human S100b to calcium binding was monitored by ^{1}H NMR spectroscopy. As shown in Figure 2A, the aromatic region of apo-S100b contains several well-resolved resonances between 5.9 and 7.5 ppm. In the apo-form of S100b, the most upfield of these resonances correspond to F70ζ, F73δ, F70δ, F14δ, and Y17ϵ as determined from the ^{1}H assignment of human S100b (Smith and Shaw, unpublished results). Upon addition of calcium to apo-S100b (Figure 2B), these resonances decrease in size with minimal line broadening typical of slow exchange. Further calcium addition resulted in the appearance of some new resonances, including F14δ, F70δ, and F70ζ which were shifted upfield of their positions in the apo-protein. These resonances were much broader in line width in the calcium form than in apo-S100b. In addition, it was also clear that at least one resonance, Y17ϵ, remained at the same position in Ca-S100b as in apo-S100b. Additions of calcium past 4 equiv did not result in narrowing of the Ca-S100b resonances. These calcium-induced spectral changes of S100b, shown in Figure 2, suggest that calcium is binding to the protein and is promoting a structural change resulting in an increase in the line width for some of the resonances in the calcium form of the protein only.

In order to monitor local structural changes from calcium binding to S100b, calcium additions were performed on a protein labeled specifically with [^{15}N]glycine produced using an *E. coli* auxotroph. Human S100b contains four glycine residues located at positions 19 and 22 in the N-terminal pseudo-calcium-binding loop and at positions 64 and 66 in the C-terminal EF-hand. Figure 3A shows a ^{1}H−^{15}N HSQC spectrum of uniformly ^{15}N-labeled S100b in the absence of calcium. The HSQC spectrum for specifically ^{15}N-labeled glycine S100b is shown in Figure 3B. In this latter spectrum, the four distinct glycine resonances are present in the top portion of the spectrum. In addition, three of the four serine residues in S100b, which were also ^{15}N-labeled, are identified. Upon calcium addition (Figure 3C) to the [^{15}N]glycine-labeled protein, the four glycine resonances decreased in intensity simultaneously as did the three serine resonances. At increased calcium concentrations, peaks corresponding to the Ca-S100b form appeared at positions different from those of the apo-protein. As was observed with the ^{1}H spectra (Figure 2), these new peaks were also accompanied by resonance broadening. Assignment of the glycine resonances in Ca-S100b was accomplished by sequential assignment from ^{15}N NOESY-HSQC spectra (Smith and Shaw, unpublished results). While all the resonances shifted in response to calcium binding, it was clear that the largest change occurred for G66, found in the C-terminal calcium-binding loop, which moved 2.1 ppm in ^{1}H chemical shift and 5 ppm in ^{15}N chemical shift.

Potassium-Induced Changes in ^{1}H Spectra. To determine the origins of the line broadening in Ca-S100b, the influence of KCl concentration on line width was examined. It has been previously determined that KCl has an antagonistic effect for calcium binding to S100b and has been suggested

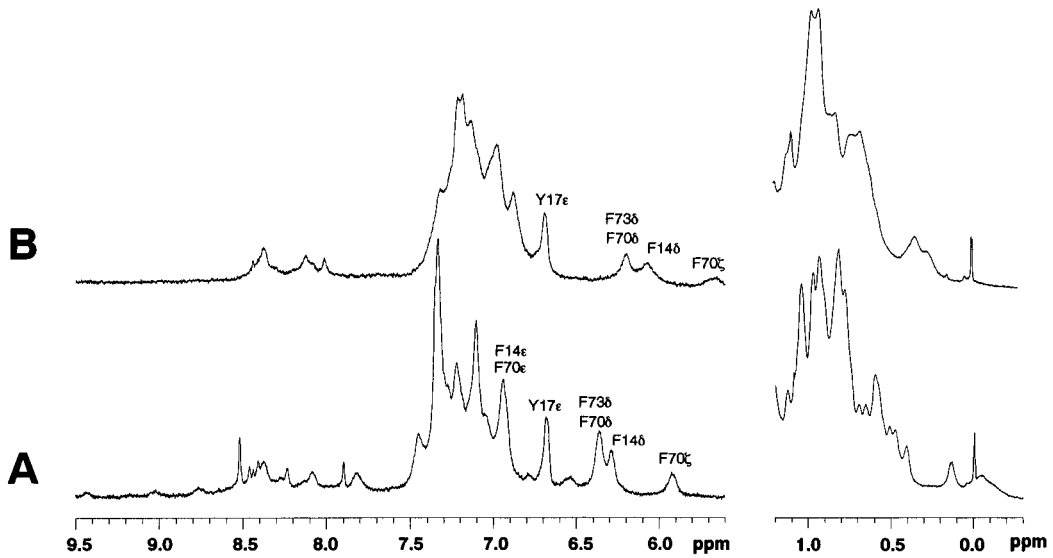

FIGURE 2: Aromatic regions from the 500-MHz ^{1}H NMR spectra of 0.22 mM recombinant human S100b in the apo (A) and calcium-bound (B) forms in D_2O, 30 mM KCl, and 20 mM imidazole-d_4 at 35 °C. In (A), some small resonances from backbone amide protons remain because of incomplete hydrogen exchange. The calcium-bound form of S100b (B) represents the spectrum where the Ca/protein ratio is approximately 4:1. Assignments for the apo species were made via a variety of 3-D heteronuclear NMR techniques and are shown above each spectrum. All other conditions are described under Materials and Methods.

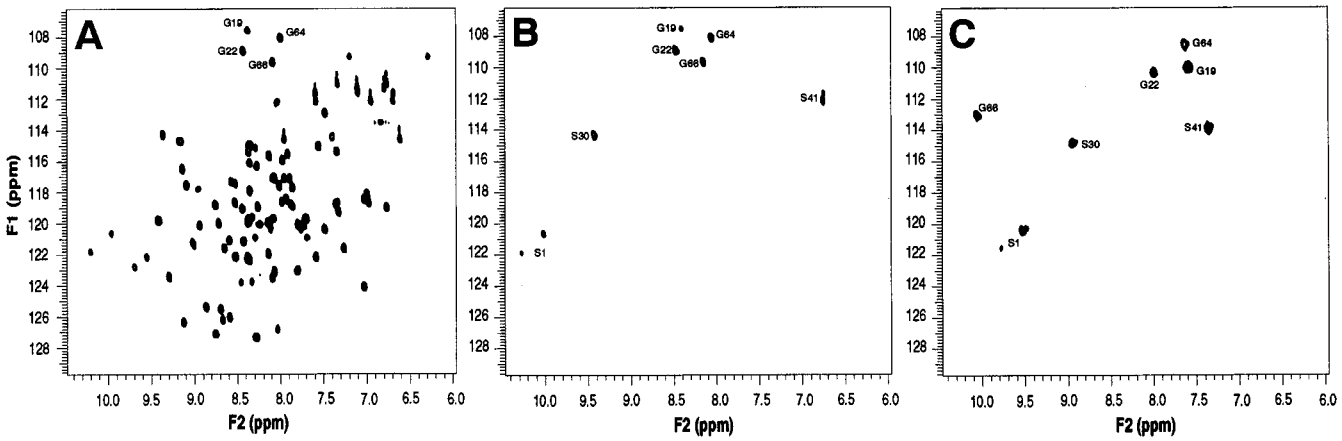

FIGURE 3: 500-MHz $^1H-^{15}N$ HSQC NMR spectra of ^{15}N uniformly and glycine selectively labeled human S100b in 90% H_2O/10% D_2O, 30 mM KCl, and 20 mM imidazole-d_4 at 35 °C. The spectra show (A) 0.5 mM ^{15}N uniformly labeled apo-S100b, (B) 0.4 mM selectively labeled [^{15}N]glycine apo-S100b, and (C) 0.4 mM selectively labeled [^{15}N]glycine S100b in the presence of 3.8 mM calcium and 10% (v/v) TFE. The four glycine residues in the apo and calcium-bound species are labeled in each spectrum and were assigned using 3-D heteronuclear NMR techniques. G19 and G22 are located in the N-terminal pseudo-EF hand calcium binding loop whereas G64 and G66 are located in the C-terminal EF-hand. All other conditions are described under Materials and Methods.

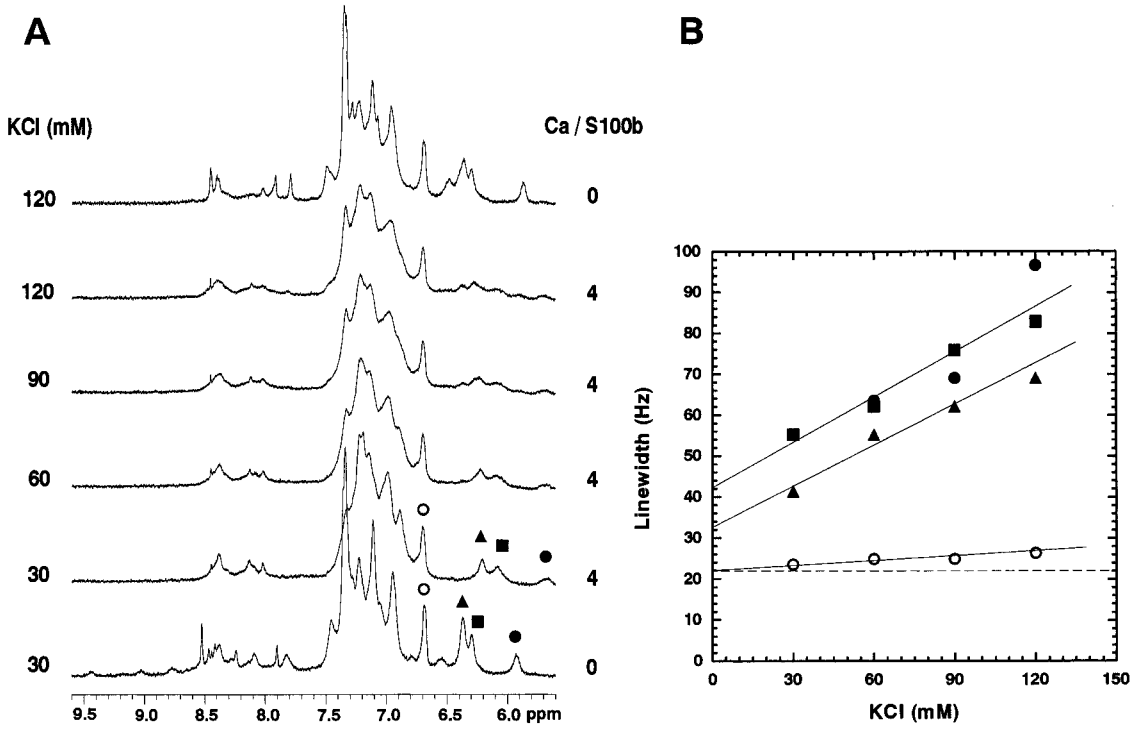

FIGURE 4: (A) Aromatic regions of 500-MHz ^1H NMR spectra showing the effects of ionic strength on apo- and calcium-bound human S100b in D_2O at 35 °C. The lower spectrum shows 0.22 mM apo-S100b in the presence of 30 mM KCl. The next four spectra show 0.22 mM S100b (Ca/S100b ratio approximately 4:1) for the following KCl concentrations: 30 mM, 60 mM, 90 mM, and 120 mM as indicated in the side legend. The top spectrum shows apo-S100b at 120 mM KCl which was generated from the addition of 2.5 mM EDTA to the previous sample. Several resonances in the apo and calcium forms of S100b are indicated by symbols: Y17ϵ (○); F14δ (■); F73δ and F70δ (▲); and F70ζ (●). (B) Plot of peak line width in Ca-S100b as a function of KCl concentration. The line widths of the peaks marked in (A) were measured at half-height for the spectra between 30 and 120 mM KCl and plotted using the same symbols as in (A). The dashed line represents the line width for Y17ϵ in apo-S100b, taken from the lower spectrum in (A).

to reverse the exposure of at least one phenylalanine residue in the calcium-bound form (Mani et al., 1982, 1983). A study of effects of the sequential additions of KCl on protein structure has not been previously reported. The addition of KCl to human S100b was monitored by ^1H NMR spectroscopy in the absence and presence of calcium (Figure 4A). The bottom spectrum shows the aromatic region for apo-S100b at 30 mM KCl. This spectrum is similar to that obtained in Figure 2A and shows the most upfield resonances for F70ζ, F73δ, F70δ, F14δ, and Y17ϵ. Upon calcium addition (second spectrum from bottom), the spectrum showed the same calcium-induced changes as seen in Figure 2, including significant broadening of most resonances. It is also clear from these spectra that addition of calcium has a marked effect on the intensity of the residual amide resonances. For example, residual amide peaks at $\delta > 7.6$ ppm found in apo-S100b (bottom spectrum) are reduced in number and size upon calcium addition, suggesting more rapid exchange may be present in the calcium form of the protein. However, this exchange may also be a function of the normal exchange occurring in the D_2O solution during the course of the experiment. Incremental increases in the

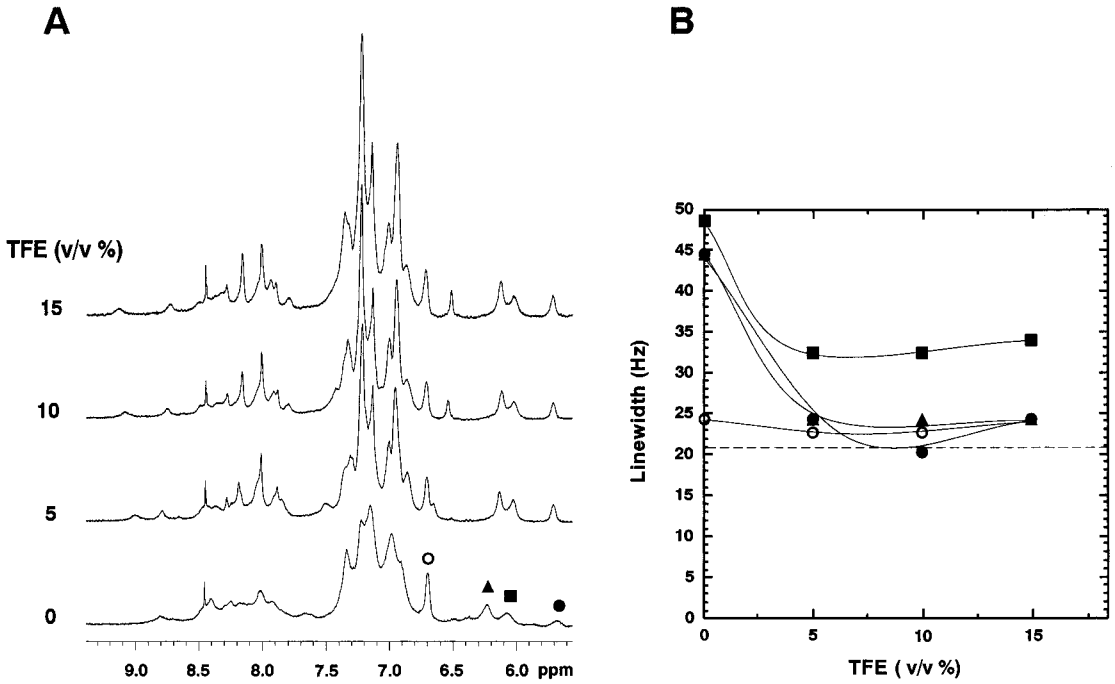

FIGURE 5: (A) Aromatic regions of 500-MHz ^{1}H NMR spectra showing the effects of trifluoroethanol (TFE) on calcium-bound human S100b in D_2O at 35 °C. The spectra show 0.22 mM Ca-S100b (Ca/S100b ratio approximately 4:1) at 50 mM KCl for TFE concentrations ranging from 0.0 to 15.0% (v/v) as indicated in the side legend. Some assigned resonances in calcium-S100b are indicated by symbols: Y17ϵ (○); F14δ (■); F73δ and F70δ (▲); and F70ζ (●). (B) Plot of peak line width in Ca-S100b as a function of TFE concentration. The line widths of the peaks marked in (A) were measured at half-height for each of the four spectra and plotted using the same symbols as in (A). The dashed line represents the line width for Y17ϵ in apo-S100b, taken from the lower spectrum in (A).

KCl concentration of the buffer (next three spectra) further broadened some of the resonances of the Ca-S100b species. As shown in Figure 4B, resonances for F70δ (▲) and F14δ (■) in Ca-S100b increase in line width by approximately 50% between 30 and 120 mM KCl. These figures also show that Y17ϵ (○) is unaffected by the increased KCl concentration. In addition, no obvious shifting of resonances nor appearance of resonances corresponding to the apo species was observed during any of these experiments. After the highest level of KCl was tested (120 mM), calcium was purged from the protein through addition of EDTA, causing the spectrum to revert back to that of apo-S100b at 120 mM KCl. A comparison of this spectrum (top) with that of the apo-protein at 30 mM KCl (bottom) showed only small changes in chemical shift of a few resonances and minimal changes in line width.

TFE-Induced Changes in ^{1}H Spectra. Increased salt concentrations have been shown to cause aggregation and solubility problems with proteins, such as cytochrome *c* and the gene V protein (Folkers et al., 1991; Whitford et al., 1991). This can be a result of an increased hydrophobic component for the protein. Since S100b exhibits differential line broadening in the calcium form only, this suggested that its hydrophobic nature is more important in the calcium form. To account for the selective line broadening in the Ca-S100b spectra, small additions of the hydrophobic solvent TFE were made to a calcium-saturated protein sample in buffer containing 30 mM KCl. At relatively high concentrations (>40% v/v), TFE can be generally categorized as a helix-stabilizing solvent which has been used frequently for the induction of structure in synthetic peptides (Lehrman et al., 1990; Marion et al., 1988). Alternatively, TFE and other solvents such as DMSO and $CHCl_3/CH_3OH$ have been used to solubilize hydrophobic membrane proteins and peptides which are insoluble in aqueous solution (Girvin & Fillingame, 1993; Orekhov et al., 1994). However, lower concentrations of TFE (<20% v/v) have been used successfully to relieve protein association resulting from hydrophobic interactions between protein molecules (Lau et al., 1984a,b; Slupsky et al., 1995a).

The effect of TFE on the ^{1}H line width of Ca-S100b was assessed by adding incremental amounts of TFE to a solution of Ca-S100b at 30 mM KCl, where we observed line broadening compared to apo-S100b. The resulting ^{1}H NMR spectra (Figure 5A) show that the addition of small amounts of TFE (<10% v/v) resulted in the sharpening of most broadened resonances in the spectrum. As shown in Figure 5B, the observed peak narrowing was most affected near 5% (v/v) TFE, and only minor improvements resulted upon further addition of the co-solvent. For example, resonances for F70δ (▲) and F70ζ (■) in calcium-S100b decrease in line width from approximately 45−50 Hz to about 25 Hz with the addition of TFE (Figure 5A, second from bottom) compared to spectra without this solvent (Figure 5A, bottom). Some resonances were insensitive to the addition of TFE, including Y17ϵ (○). This resonance remained at the same chemical shift and of the same intensity (Figure 5A,B), indicating that TFE did not affect all residues in the protein. Some shifting of resonances occurred with the increased addition of TFE. While this may be due to TFE altering the environment of certain residues, it has also been shown that some amide resonances are particularly susceptible to TFE and respond with large chemical shift changes which are a function of TFE concentration (Merutka et al., 1995).

Surface Accessibility to HyTEMPO. To assess whether calcium binding to S100b modified the surface exposure of some of the identified aromatic residues, HyTEMPO was added to solutions of the protein in the absence and presence of calcium. The approach relies on an increase in the relaxation rates of protons near the free radical HyTEMPO

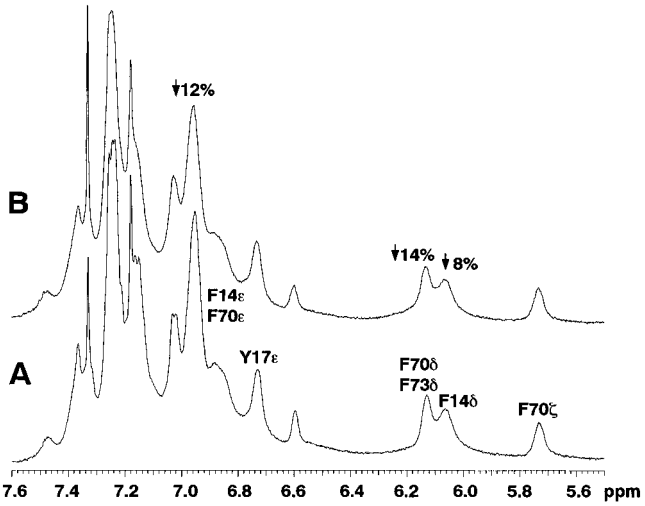

FIGURE 6: Effect of HyTEMPO on the Ca-S100b ^{1}H NMR spectrum. (A) Aromatic region of 0.2 mM Ca-S100b in 20 mM imidazole-d_4, 30 mM KCl, 10% TFE-d_3, and 90% D_2O at 35 °C. Assigned resonances in Ca-S100b are indicated above the peak. (B) Ca-S100b sample shown in (A) with 4 equiv of HyTEMPO added directly to the NMR sample. Indicated above F14δ, F73δ and F14ϵ, F73ϵ are the percentage decrease in peak height upon addition of the spin-label. No change was observed for F14ζ or Y17ϵ within the 2% measuring error of the spectra.

probe and effectively broadens the respective resonances. In the case of protein−ligand complexes, HyTEMPO can be covalently attached to the ligand, which upon tight binding to the protein can dramatically increase relaxation rates to the extent that resonances near the probe become significantly broadened and difficult to resolve from the spectrum base line (Yu et al., 1994; Zhang et al., 1995b). On the other hand, HyTEMPO can also help identify surface residues through nonspecific collision with the protein. This can lead to more subtle changes in the line width of any affected resonances (Petros et al., 1990; Esposito et al., 1992) or the respective relaxation rates (Cocco et al., 1994; Howarth et al., 1995).

HyTEMPO was added to both apo-S100b and Ca-S100b, and the resulting ^{1}H NMR spectra were analyzed for small amounts of line broadening which would indicate which residues are at least partly surface-exposed (Petros et al., 1990; Esposito et al., 1992). In Figure 6, the aromatic regions on the ^{1}H NMR spectra are shown in the presence of calcium and/or 4 equiv HyTEMPO. This ratio of HyTEMPO was selected to offset the 4 reducing equiv of the reduced cysteine residues in S100b. It was also consistent with HyTEMPO/protein ratios used in similar experiments with ubiquitin and lysozyme where 4−6 equiv of HyTEMPO was typically used (Petros et al., 1990; Esposito et al., 1992). The apo-S100b spectra showed that F70ζ was the only observable resonance affected by HyTEMPO addition, having an approximate decrease in peak intensity of about 10%. In Ca-S100b, small decreases in peak intensity were noted for F14δ (8%) and F73δ (14%) while no change was noted in F70ζ. In this analysis, the lack of broadening in F70ζ in Ca-S100b was interpreted to indicate that broadening of the resonance near 6.1 ppm was a result of F73δ broadening only. Other resonances are seen to broaden in this spectrum but at this time have not been identified.

DISCUSSION

Previous studies utilizing CD and absorption difference spectroscopies have provided useful structural insights into the calcium induced conformational changes in S100b. These data have shown that calcium binding to S100b perturbs at least one of the aromatic residues in the protein (Mani et al., 1982, 1983). Further, it has been observed that increased ionic strength also leads to a structural modification in the calcium form of S100b, which also appears to involve aromatic residues (Mani et al., 1982, 1983). In this past work, determination of the precise residues affected by calcium binding or ionic strength was not possible. The recent three-dimensional structure of apo-calcyclin (Potts et al., 1995) now allows the effects of calcium binding on S100b to be determined in a more quantitative manner. Based on a high sequence similarity, it is likely that apo-S100b has a similar three-dimensional fold as apo-calcyclin. In particular, several hydrophobic residues are strictly conserved in S100b including F14, F70, F73, F76, and F88. In the present work, we have focused on the glycine and some phenylalanine residues in human S100b and used NMR spectroscopy to determine which of these are most sensitive to calcium binding and ionic strength. These have been rationalized based on comparisons with the apo-calcyclin structure.

Calcium-Dependent Conformational Changes. The data in Figure 2 show that several of the aromatic ^{1}H resonances are affected by calcium binding to human S100b. In combination with previous difference absorption and CD spectroscopy, this result confirms a calcium-sensitive conformational change in S100b. Specifically, the ^{1}H NMR spectra in Figures 2 and 4 show that the side chain resonances from the aromatic residues F14, F70, and F73 shift and broaden in response to calcium binding. These residues are located toward the proposed N-terminal helix (F14) and in the C-terminus of the site II calcium-binding site (F70, F73). The upfield shifts of these resonances in Ca-S100b are similar to those observed in calbindin D_{9k} for the analogous residues (F10, F63, F67), where the side chains of these aromatics are stacked and undergo only a slight rearrangement upon calcium binding (Kordel et al., 1993). However, unlike S100b, in calbindin D_{9k} no broadening of the resonances occurs, and the changes in chemical shift are smaller. In addition, the position of F70ζ in S100b (5.91 ppm in apo-S100b) is significantly different compared to the equivalent position in calbindin D_{9k} (F63, 7.31ppm) (Skelton et al., 1990), likely reflecting an important difference in environment. For S100b, better insight into the calcium-induced structural changes may be obtained from the recent low-resolution solution structure of apo-calcyclin, a dimeric member of the S100 protein family (Potts et al., 1995). In this structure, a hydrophobic core is present at the interface of the two monomers which includes F16, F70, and L88 (in S100b, the analogous residues are F14, F70, and F88). If apo-S100b has a similar structure to apo-calcyclin, then the changes in chemical shift and broadening for F70, F73, and F14 are suggestive that the packing of these residues is perturbed during calcium binding.

The ^{1}H NMR data in Figure 2 show that the resonance for Y17ϵ is insensitive to calcium binding and that little rearrangement of Y17 occurs upon calcium binding in S100b. In the structure of apo-calcyclin, the analogous residue Y19

is predominantly buried and has an approximate 15% exposure to solvent (Potts et al., 1995). Likewise, Y13 in calbindin D_{9k} is hydrogen-bonded to E35 in both the apo- and calcium forms of calbindin D_{9k} and undergoes little change in exposure to solvent (Skelton et al., 1994). ^{1}H NMR data also show that the resonance for Y13ϵ in calbindin D_{9k} is not affected by calcium binding (Linse et al., 1987). Combining these observations, our data indicate that Y17 in both apo-S100b and Ca-S100b forms maintains a position similar to that in the apo-calcyclin structure. This interpretation differs from conclusions reached from earlier absorption difference and fluorescence spectra which indicated that calcium binding perturbed Y17 in S100b either by moving it to a more protected environment (Mani et al., 1982, 1983) or by promoting a hydrogen bond between the hydroxyl of Y17 and a close carboxyl acceptor (Baudier & Cole, 1989).

The use of [^{15}N]glycine in S100b provided an excellent nonperturbing NMR probe for calcium binding in S100b since two glycine residues are present in each calcium-binding loop (G19, G22 in site I and G64, G66 in site II). As shown in Figure 3, all four glycine resonances change chemical shift upon calcium binding, but to different degrees. The glycine resonance most affected is G66 which moves significantly downfield in both ^{1}H and ^{15}N frequencies. The resulting NH ^{1}H frequency for G66 (10.08 ppm) is very similar to that observed in Ca-TnC (10.3-10.8 ppm) (Krudy et al., 1992; Slupsky et al., 1995b), Ca-CaM (10.3−10.7 ppm) (Ikura et al., 1990), and G59 in site II of Ca-calbindin D_{9k} (10.6 ppm) (Kördel et al., 1989). This glycine participates in a canonical EF-hand loop structure as has been observed in the X-ray structures of these latter proteins (Babu et al., 1988; Herzberg & James, 1988; Szebenyi & Moffat, 1986) forming a central hinge in the calcium-binding loop. In calbindin D_{9k}, this includes a hydrogen bond from G59 NH back to the carbonyl of G57 (Szebenyi & Moffat, 1986). The large downfield shift of G66NH is indicative that G66 acts as a hinge residue in site II.

A comparison of the calcium-induced chemical shift changes for G19 and G22 in the site I calcium-binding loop of S100b with those of glycine residues in calbindin D_{9k} (G18, G57) reveals a remarkable similarity. For example, the NH and ^{15}N resonances for G22 in S100b both shift downfield upon calcium binding (NH, from 8.43 to 9.04 ppm; ^{15}N, from 108.91 to 115.08 ppm) while the NH resonance for G64 in S100b shifts upfield and its ^{15}N resonance shifts downfield. Both of these trends are nearly identical to those observed in calbindin D_{9k} (Kördel et al., 1989; Skelton et al., 1990, Skelton et al., 1992). Overall, these results show that calcium binding to recombinant S100b results in a similar conformational change in the calcium-binding loops as in calbindin D_{9k}. However, the calcium-induced broadening of resonances for F14, F70, and F73 in S100b indicates that there are differences between the proteins on the effect of calcium on some hydrophobic residues in the N- and C-terminal regions.

Protein Association via a Hydrophobic Surface in S100b. Calcium binding causes significant line broadening of several resonances in Ca-S100b only. The lack of observable broadening of resonances from the apo-S100b species indicates that this broadening is not a result of exchange with the metal ion. Rather, it implies that regions of Ca-S100b are motionally restricted compared to the apo-protein. The increase in the ^{1}H line widths in Ca-S100b as a function of ionic strength shows that a hydrophobic component in Ca-S100b is responsible for these observations. Similar conclusions have been reached for other proteins and have been attributed to protein association or aggregation (Folkers et al., 1991; Whitford et al., 1991).

Recently, it has been shown that TFE can interact with the surface residues on proteins to relieve hydrophobic protein−protein association. In the calcium-binding protein troponin-C, TFE has been used to reverse a dimerization of the protein via exposed hydrophobes in the N-terminal domain of the protein, while not affecting the secondary or tertiary structure of the protein (Slupsky et al., 1995a). As a result, ^{1}H and ^{15}N line widths in the N-terminal domain of calcium-saturated troponin-C (15% TFE) were decreased by approximately 50% compared to the same peaks in the absence of TFE. These previous findings are very similar to our current work where resonances for the side chains of F70, F73, and F14 broaden in the presence of calcium and can be narrowed by additions of small amounts of TFE (Figure 5). In Ca-S100b, this combination of increased line width from increasing amounts of KCl and the beneficial effect of TFE show that hydrophobic interactions form the basis for motional restriction which is magnified at increased ionic strength. This also shows that the increased ionic strength does not simply result in electrostatic screening of the calcium ions.

The calcium-induced conformational changes which occur in human S100b can be assessed based on the observations here, the three-dimensional structure of apo-calcyclin, and the detailed and well-understood conformational changes that occur in calbindin D_{9k}. These three proteins share a high degree of sequence similarity including residues F14, Y17, F60, and F63. The average NMR structure of apo-calbindin D_{9k} shows that F10 and F66 are both protected from solvent whereas F63 is partially exposed (Skelton et al., 1995). Calcium binding to this protein causes a rigid-body motion of helix III and a reorganization of packing of this helix with helix IV and with helices I and II (Skelton et al., 1994, 1995). For example, changes in position of F63 and F66 affect F10 and changes in V70 affect L6 and F36. Overall, no modification in the exposure of any of these hydrophobic residues accompanies calcium binding with the exception of a small increase in exposure of F63. In the apo-calcyclin structure, homologous residues to calbindin D_{9k} form the hydrophobic core including three residues, F14, F70, and Y73, which form intermonomer contacts at the dimer interface with F88 (Potts et al., 1995). In particular, F88 has been suggested to be the anchor for this cluster and represents a residue in the sequence of S100b which is not present in the calbindin D_{9k} sequence (Potts et al., 1995). One significant difference between these proteins is that F70 is completely buried in apo-calcyclin whereas the analogous residue, F63, in apo-calbindin is partially exposed and becomes more exposed upon calcium binding.

It is clear that in human apo-S100b, like apo-calcyclin, an intimate association of residues F14, F70, F73, and F88 exists. Of these residues, F14, F70, and F73 broaden upon calcium binding, are adversely affected by KCl, and decrease in line width upon addition of TFE. In addition, we have observed that the ^{1}H−^{15}N resonance for F88 undergoes a significant calcium-induced change in chemical shift in HSQC spectra (Smith et al., unpublished results). These

observations provide evidence that the dimer interface in S100b, comprised of F14, F70, F73, and F88, or a region nearby is rearranged upon calcium binding. The results of the HyTEMPO experiments support this idea. Even in the presence of TFE which may protect an exposed hydrophobic surface, resonances for F14 and F73 are broadened in Ca-S100b. The extent of broadening is consistent with similar small changes observed in calcium-bound cardiac TnC (Howarth et al., 1995), lysozyme, and ubiquitin (Petros et al., 1990; Esposito et al., 1992) upon addition of HyTEMPO and indicates that these residues in Ca-S100b are at least partly exposed. It is possible that F88 may also be involved although further experiments are required to confirm this. These observations are in agreement with previous absorption and CD spectroscopic results which indicate that at least one phenylalanine is exposed upon calcium binding to S100b (Mani et al., 1982, 1983). In the absence of TFE, the exposure of these residues causes a calcium-induced dimerization (possibly forming a tetramer) in analogy to observations with TnC. Support for this idea has been obtained from preliminary sedimentation equilibrium experiments where Ca-S100b (120 mM) has a higher apparent molecular mass (31 kDa) than expected from the dimeric species (21 kDa) (Smith et al., unpublished results). These observations are reinforced from small-angle X-ray scattering experiments which show that S100b forms an aggregated species in solution (Matsuda et al., 1993).

A calcium-induced structural change involving F14, F73, and F88 is consistent with the hypothesis that S100b undergoes a calcium-sensitive conformational change, exposing a hydrophobic region, enabling it to interact with a nonpolar region on a target protein (Heizmann & Hunziker, 1991; Hilt & Kligman, 1991). It is interesting that F88 in the S100 protein p11 has been implicated as an important residue for its interaction with annexin II (Kube et al., 1992). It has further been proposed that C84 becomes exposed in S100b upon calcium binding (Baudier et al., 1986a). Another mechanism whereby S100b may function is via a calcium-induced dimerization of the protein. In the dimeric S100 proteins calgranulins A and B, it has been observed that calcium binding induces protein association where trimeric and tetrameric species are formed (Teigelkamp et al., 1991). This is thought to be important for translocation of these proteins to the plasma membrane. A similar mechanism may operate for S100b as it has been shown that S100b is found at the plasma membrane of glial cells (Donato et al., 1989; Rambotti et al., 1990).

ACKNOWLEDGMENT

We thank one of the reviewers for suggesting the HyTEMPO experiment. We also thank Lewis Kay (University of Toronto) for advice on NMR experiments and providing the gradient-HSQC pulse sequence. We are grateful to Lawrence McIntosh (University of British Columbia) for the gift of auxotrophic *E. coli* strains and his suggestions for ^{15}N labeling. The coordinates for the S100b model mentioned in this paper were generously provided by Walter Chazin and Barbara Potts (Scripps Institute, La Jolla, CA).

REFERENCES

Akke, M., Drakenberg, T., & Chazin, W. (1992) *Biochemistry 31*, 1011−1020.
Babu, Y. S., Bugg, C. E., & Cook, W. J. (1988) *J. Mol. Biol. 203*, 191−204.
Baudier, J., & Gerard, D. (1983) *Biochemistry 22*, 3360−3369.
Baudier, J., & Cole, R. D. (1989) *Biochem. J. 264*, 79−85.
Baudier, J., Glasser, N., Haglid, K., & Gerard, D. (1984) *Biochim. Biophys. Acta 790*, 164−173.
Baudier, J., Labourette, G., & Gerard, D. (1985) *J. Neurochem. 44*, 76−84.
Baudier, J., Glasser, N., & Duportail, G. (1986a) *Biochemistry 25*, 6934−6941.
Baudier, J., Glasser, N., & Gerard, D. (1986b) *J. Biol. Chem. 261*, 8192−8203.
Baudier, J., Mochly-Rosen, D., Newton, A., Lee, S.-H., Koshland, D. E., & Cole, R. D. (1987) *Biochemistry 26*, 2886−2893.
Baudier, J., Delphin, C., Grunwald, D., Khochbin, S., & Lawrence, J. J. (1992) *Proc. Natl. Acad. Sci. U.S.A. 89*, 11627−11631.
Bianchi, R., Giambanco, I., & Donato, R. (1993) *J. Biol. Chem. 268*, 12669−12674.
Cocco, M. J., & Lecomte, J. T. J. (1994) *Protein Sci. 3*, 267−281.
Donato, R. (1988) *J. Biol. Chem. 263*, 106−110.
Donato, R., Giambanco, I., Aisa, M. C., & Ceccarelli, P. (1989) *FEBS Lett. 247*, 31−35.
Esposito, G., Lesk, A. M., Molinari, H., Motta, A., Niccolai, N., & Pastore, A. (1992) *J. Mol. Biol. 224*, 659−670.
Finn, B. E., Evenas, J., Drakenberg, T., Walthro, J. P., Thulin, E., & Forsen, S. (1995) *Nat. Struct. Biol. 2*, 777−783.
Folkers, P. J. M., Stassen, A. P. M., van Duynhoven, J. P. M., Harmsen, B. J. M., Konings, R. N. H., & Hilbers, C. W. (1991) *Eur. J. Biochem. 200*, 139−148.
Gagne, S. M., Tsuda, S., Li, M. X., Chandra, M., Smillie, L. B., & Sykes, B. D. (1994) *Protein Sci. 3*, 1961−1974.
Gagne, S. M., Tsuda, S., Li, M. X., Smillie, L. B., & Sykes, B. D. (1995) *Nat. Struct. Biol. 2*, 784−789.
Girvin, M. E., & Fillingame, R. H. (1993) *Biochemistry 32*, 12167−12177.
Heizmann, C. W., & Hunziker, W. (1991) *Trends Biochem. Sci. 16*, 98−103.
Herzberg, O., & James, M. N. G. (1988) *J. Mol. Biol. 203*, 761−779.
Hilt, D. C., & Kligman, D. (1991) in *Novel Calcium-Binding Proteins. Fundamentals and Clinical Implications* (Heinzmann, C. W., Ed.). pp 65−103, Springer-Verlag, Berlin.
Howarth, J. W., Krudy, G. A., Lin, X., Putkey, J. A., & Rosevear, P. R. (1995) *Protein Sci. 4*, 671−680.
Ikura, M., Kay, L. E., & Bax, A. (1990) *Biochemistry 29*, 4659−4667.
Isobe, T., & Okuyama, T. (1981) *Eur. J. Biochem. 116*, 79−86.
Ivanenkov, V. V., Jamieson, G. A., Gruenstein, E., & Dimlich, R. V. W. (1995) *J. Biol. Chem. 270*, 14651−14658.
Kay, L. E., Keifer, P., & Saarinen, T. (1992) *J. Am. Chem. Soc. 114*, 10663−10665.
Kördel, J., Forsén, S., & Chazin, W. J. (1989) *Biochemistry 28*, 7065−7074.
Kordel, J., Skelton, N. J., Akke, M., & Chazin, W. J. (1993) *J. Mol. Biol. 231*, 711−734.
Krudy, G. A., Brito, R. M. M., Putkey, J. A., & Rosevear, P. R. (1992) *Biochemistry 31*, 1595−1602.
Kube, E., Becker, T., Weber, K., & Gerke, V. (1992) *J. Biol. Chem. 267*, 14175−14182.
Kuboniwa, H., Tjandra, N., Grzesiek, S., Ren, H., Klee, C. B., & Bax, A. (1995) *Nat. Struct. Biol. 2*, 768−776.
Lau, S. Y. M., Taneja, A. K., & Hodges, R. S. (1984a) *J. Chromatogr. 317*, 129−140.
Lau, S. Y. M., Taneja, A. K., & Hodges, R. S. (1984b) *J. Biol. Chem. 259*, 13253−13261.
Lehrman, S. R., Tuls, J. L., & Lund, M. (1990) *Biochemistry 29*, 5590−5596.
LeMaster, D. M., & Richards, F. M. (1988) *Biochemistry 27*, 142−150.
Lin, L.-H., Van Eldik, L. J., Osheroff, N., & Norden, J. J. (1994) *Mol. Brain Res. 25*, 297−304.
Linse, S., Brodin, P., Drakenberg, T., Thulin, E., Sellers, P., Elmden, K., Grundstrom, T., & Forsén, S. (1987) *Biochemistry 26*, 6723−6735.
Mani, R. J., Boyes, B. E., & Kay, C. M. (1982) *Biochemistry 21*, 2607−2612.

Mani, R. S., Shelling, J. G., Sykes, B. D., & Kay, C. M. (1983) *Biochemistry 22*, 1734.
Marion, D., Zasloff, M., & Bax, A. (1988) *FEBS Lett. 227*, 21−26.
Merutka, G., Dyson, H. J., & Wright, P. E. (1995) *J. Biomol. NMR 5*, 14−24.
Muchmore, D. C., McIntosh, L. P., Russell, C. B., Anderson, D. E., & Dahlquist, F. W. (1989) in *Methods in Enzymology* (Oppenheimer, N. J., & James, T. L., Eds.) pp 44−73, Academic Press, New York.
Ogoma, Y., Kobayashi, H., Fujii, T., Kondo, Y., Hachimori, A., Shimizu, T., & Hatana, M. (1992) *Int. J. Biol. Macromol. 14*, 279−286.
Orekhov, V. Y., Pervushin, K. V., & Arseniov, A. S. (1994) *Eur. J. Biochem. 219*, 887−896.
Patel, A. M., & Dunn, S. D. (1995) *J. Bacteriol. 177*, 3917−3922.
Petros, A. M., Mueller, L., & Kopple, K. D. (1990) *Biochemistry 29*, 10041−10048.
Potts, B. C. M., Smith, J., Akke, M., Macke, T. J., Okazaki, K., Hidaka, H., Case, D. A., & Chazin, W. J. (1995) *Nat. Struct. Biol. 2*, 790−796.
Rambotti, M. G., Sprec, A., Leoncini, P., Estenoz, M., Costantino-Ceccarini, E., Giambianco, I., & Donato, R. (1990) *J. Histochem. Cytochem. 38*, 1583−1589.
Sambrook, J., Fritsch, E. F., & Maniatis, T. (1989) *Molecular cloning: a laboratory manual*, Cold Spring Harbor Laboratory Press Cold Spring Harbor, NY.
Satyshur, K. A., Rao, S. T., Pyzalska, D., Drendel, W., Greaser, M., & Sundaralingam, M. (1988) *J. Biol. Chem. 263*, 1628−1647.
Satyshur, K. A., Pyzalska, D., Greaser, M., Rao, S. T., & Sundaralingam, M. (1994) *Acta Crystallogr. D50*, 40−49.
Sheu, F.-S., Huang, F. L., & Huang, K.-P. (1995) *Arch. Biochem. Biophys. 316*, 335−342.
Skelton, N. J., Forsén, S., & Chazin, W. J. (1990) *Biochemistry 29*, 5752−5761.
Skelton, N. J., Kordel, J., Akke, M., & Chazin, W. J. (1992) *J. Mol. Biol. 227*, 1100−1117.
Skelton, N. J., Kordel, J., Akke, M., Forsen, S., & Chazin, W. (1994) *Struct. Biol. 1*, 239−245.
Skelton, N. J., Kordel, J., & Chazin, W. J. (1995) *J. Mol. Biol. 249*, 441−462.
Slupsky, C. M., Kay, C. M., Reinach, F. C., Smillie, L. B., & Sykes, B. D. (1995a) *Biochemistry 34*, 7365−7375.
Slupsky, C. M., Reinach, F. C., Smillie, L. B., & Sykes, B. D. (1995b) *Protein Sci.*, 1279−1290.
Szebenyi, D. M. E., & Moffat, K. J. (1986) *J. Biol. Chem. 261*, 8761−8777.
Teigelkamp, S., Bhardwaj, R. S., Roth, J., Meinardus-Hager, G., Karas, M., & Sorg, C. (1991) *J. Biol. Chem. 266*, 13462−13467.
VanEldik, L. J., Staecker, J. L., & Winningham-Major, F. (1988) *J. Biol. Chem. 263*, 7830−7837.
Whitford, D., Concar, D. W., & Williams, R. J. P. (1991) *Eur. J. Biochem. 199*, 561−568.
Williams, T. C., Corson, D. C., Oikawa, K., McCubbin, W. D., Kay, C. M., & Sykes, B. D. (1986) *Biochemistry 25*, 1835−1846.
Wishart, D. S., Sykes, B. D., & Richards, F. M. (1992) *Biochemistry 31*, 1647−1651.
Yu, L., Meadows, R. P., Wagner, R., & Fesik, S. W. (1994) *J. Magn. Reson. B104*, 77−80.
Zhang, M., Tanaka, T., & Ikura, M. (1995a) *Nat. Struct. Biol. 2*, 758−767.
Zhang, M., Yuan, T., Aramini, J., & Vogel, H. J. (1995b) *J. Biol. Chem. 270*, 20901−20907.

BI952698C